D-allose enhances the efficacy of hydroxychloroquine against Lewis lung carcinoma cell growth by inducing autophagy

KYOKA YAMAZAKI[1,2], MASATO HOSHI[3], HIROYUKI TEZUKA[4], NANAKA MORITA[1], MASAYA HIRAYAMA[5], FUMIAKI SATO[3], SAYAKA YOSHIDA[3] and KUNIAKI SAITO[1]

[1]Department of Disease Control and Prevention, Fujita Health University, Aichi 470-1192; [2]Research and Development, Matsutani Chemical Industry Co., Ltd., Hyogo 664-8508; Departments of [3]Informative Clinical Medicine, [4]Cellular Function Analysis, Research Promotion Headquarters, and [5]Morphology and Diagnostic Pathology, Fujita Health University, Aichi 470-1192, Japan

Received November 5, 2021; Accepted April 5, 2022

DOI: 10.3892/or.2022.8328

Abstract. Various cancer cells require massive amounts of glucose as an energy source for their dysregulated growth. Although D-allose, a rare sugar, inhibits tumor cell growth via inhibition of glucose uptake, a few cells can survive after treatment. However, the mechanism by which D-allose-resistant cells are generated remains unclear. Here, we investigated the properties of D-allose-resistant cells and evaluated the efficacy of combined treatment with this rare sugar and antitumor drugs. To this end, we established a D-allose-resistant tumor cell line and prepared a C57BL/6J mouse tumor xenograft model using Lewis lung carcinoma (LLC) cells. Xenograft-bearing mice were treated with D-allose (9 g/kg) and/or hydroxychloroquine (HCQ, 60 mg/kg), an autophagy inhibitor, for two weeks. Although D-allose inhibited LLC cell growth in a dose-dependent manner, a few cells survived. The upregulation of LC3-II, a classical autophagy marker, and the downregulation of mTOR and its downstream molecule Beclin1 were observed in established D-allose-resistant LLC cells, which were more sensitive to cell death induced by HCQ. Similarly, in the tumor xenograft model, the tumor volume in mice co-treated with D-allose and HCQ was considerably smaller than that in untreated or HCQ-treated mice. Importantly, the administration of D-allose induced autophagy selectively at the tumor site of the xenograft-bearing mice. These results provide a new therapeutic strategy targeting autophagy which is induced in tumor cells by D-allose administration, and may be used to improve therapies for lung cancer.

Correspondence to: Dr Masato Hoshi, Department of Informative Clinical Medicine, Fujita Health University, 1-98 Dengakugakubo, Kutsukake-cho, Toyoake, Aichi 470-1192, Japan
E-mail: mhoshi@fujita-hu.ac.jp

Key words: D-allose, autophagy, rare sugar, Lewis lung carcinoma cells, hydroxychloroquine

Introduction

Lung cancer is associated with high morbidity and mortality worldwide, with 1.8 million estimated deaths due to lung cancer as a primary condition in 2020 (1). Current treatments for lung cancer include resection of the tumor site, radiation therapy, and for treating advanced cancers, platinum-based chemotherapy and multi-drug combinations such as immune checkpoint inhibitors are used. However, the five-year survival rate has been reported to be approximately 19%, and lung cancer remains one of the most intractable cancers (2). Therefore, despite the implementation of these therapies, sufficient therapeutic efficacy has yet to be achieved, suggesting that the underlying mechanisms of lung cancer treatment remain to be elucidated. Determining the mechanisms that differ from those of conventional therapeutic target molecules will enable us to develop novel therapeutic strategies for patients with lung cancer who do not respond to current therapies.

Recently, the use of rare sugars that are defined as monosaccharides and their rare derivatives has attracted attention for their various physiological functions. Among these sugars, D-allose has a sweetness of 80% compared to that of sugar (3), is not readily used as an energy source (4), and is safe for consumption by mammals (5). D-allose was reported to protect against post-ischemic reperfusion injury in a gerbil and rat model (6), and it arrests the cell cycle from the G1 to S phase via stabilization of cyclin-dependent kinase inhibitor 1 B (also called p27kip1) (7). Notably, D-allose increases thioredoxin-interacting protein (TXNIP) levels, a negative regulator of glucose transporter 1 (GLUT1), and inhibits tumor cell growth via inhibition of glucose uptake (8,9). The antitumor efficacy of D-allose has been observed in combination with chemotherapy or radiation therapy in a carcinoma mouse model (10). However, the tumor was not completely removed after treatment with D-allose alone or in combination with chemotherapy or radiation therapy (8-10), implying the generation of D-allose-resistant tumor cells.

Tumor cells have acquired numerous functions to enable their survival under hypoxic and hypotrophic conditions in the microenvironment. For example, under hypoxic conditions, tumor cells adapt to the microenvironment by increasing the

expression of hypoxia-inducible factor-1 (HIF-1) (11). Under hypotrophic conditions, tumor cells induce autophagy to survive during nutrient starvation involving glucose deprivation, via the induction of mTOR (12-16). Therefore, a strategy for cancer treatment that targets glucose metabolism alone is not sufficient; it is important to simultaneously regulate the accompanying evasion mechanisms such as autophagy.

In the present study, we found that although D-allose killed most of the tumor cells, a few cells induced autophagy to survive. Furthermore, we showed that a combined treatment with D-allose and the autophagy inhibitor hydroxychloroquine (HCQ) significantly suppressed tumor cell growth without any side effects in a mouse tumor model.

Materials and methods

Chemicals. The monosaccharides used in this study are listed in Table I. D-glucose was purchased from Nacalai Tesque, and D-mannose, D-allose, D-psicose, D-tagatose, D-sorbose, L-psicose, D-arabinose, L-arabinose, and L-fucose were obtained from Matsutani Chemical Industry Co., Ltd. Hydroxychloroquine (HCQ) sulfate was purchased from Sigma-Aldrich/Merck KGaA (catalog no. H0915).

Cell culture. Mouse Lewis lung carcinoma (LLC) cells were purchased from Riken BioResource Center (catalog no. RCB0558, RRID: CVCL_4358) and mouse skin melanoma (B16F10) cells were obtained from the American Type Culture Collection (ATCC) (catalog no. CRL-6475). The MDA-MB-231 human breast adenocarcinoma cell line was purchased from the Japanese Cancer Research Resources Bank (catalog no. JCRB1559). LLC, B16F10, and MDA-MB-231 cells were maintained in RPMI-1640 or low-glucose DMEM (Fujifilm Wako Pure Chemical, Ltd.) supplemented with 10% FBS (Thermo Fisher Scientific, Inc.) and penicillin (100 units/ml)-streptomycin (0.1 mg/ml) (Life Technologies/Thermo Fisher Scientific, Inc.).

The cells were given fresh culture media twice per week and were subcultured to confluency after detaching the cells with 0.25% trypsin +0.02% EDTA at a weekly split ratio of ~1:2. Cultures from passages 10 to 25 were used in all experiments. The cells were screened periodically for mycoplasma contamination using a Mycoplasma Detection kit (MycoAlert™; Lonza Group, Ltd.).

For the cell viability assay, cells ($1x10^5$/well) were seeded in 6-well plates and cultured for 24 h at 37˚C in 5% CO_2. Monosaccharides dissolved in PBS were added to form a final concentration of 25 or 50 mM. Stocks of monosaccharides (500 mM) were prepared in RPMI-1640 medium and sterilized via filtration through a 0.2-μm pore filter. For the control conditions, the same volume of PBS was added. The viable cells were enumerated via 0.5% trypan blue staining (Nacalai Tesque).

Establishment of D-allose-resistant LLC cells. D-allose-resistant LLC cells were established using the following procedure: Untreated LLC cells were seeded at a density of $2x10^4$ cells/ml in a 100-mm dish. D-allose (25 mM) dissolved in the RPMI-1640 medium was added. After 72 h, cells were harvested and enumerated via 0.5% trypan blue staining, adjusted to a density of $2x10^4$ cells/ml, and reseeded in the presence of 25 mM D-allose. The first cell count was denoted to be passage 1, and after counts until passage 10 when the cell ratio of the control LLC cells and D-allose-resistant LLC cells exceeded 100%, the population was considered to comprise D-allose-resistant cells. Furthermore, we confirmed that D-allose-resistant LLC cells were stably resistant at least until passage 10 after establishment.

Western blot analysis. The collected cells and tumor tissues were homogenized for 1 min at 4˚C using an ultrasonic homogenizer in 9 volumes of 50 mM Tris-HCl (pH 6.8) containing 1% sodium dihydrogen phosphate, 1% protease inhibitor cocktail (Nacalai Tesque), and 1% EDTA-free phosphatase inhibitor cocktail (Nacalai Tesque). The homogenized samples were centrifuged at 15,000 x g for 10 min at 4˚C. The supernatant was collected as a sample extract. The protein concentration in the sample extract was measured using a bicinchoninic acid protein assay kit (Takara). The protein for loading was prepared by adding bromophenol blue/2-mercaptoethanol corresponding to 0.1 volumes of the final sample volume. The amount of protein loaded per lane was 0.5-40 μg (0.5 μg for Akt, p-Akt, and Beclin1, 5 μg for LC3 and p62, 40 μg for mTOR and p-mTOR). The protein samples were separated via 7.5-15% gels (7.5% for p62, mTOR, and p-mTOR, 10% for Akt, p-Akt, and Beclin1, 15% for LC3). Proteins were separated via SDS-PAGE and transferred onto PVDF membranes. The membranes were blocked with 5% skimmed milk (for LC3, p62, Akt, Beclin1, and β-actin) or 5% PhosphoBLOCKER Blocking Reagent (for mTOR, p-Akt, and p-mTOR; Cell Biolabs Inc.), diluted in TBS-T for 1 h at 25˚C, and then incubated with a primary antibody. The following antibodies were used at a dilution of 1:1,000: anti-LC3A/B (catalog no. #12741; Cell Signaling Technology, Inc.), anti-SQSTM1/p62 (catalog no. #5114; Cell Signaling Technology, Inc.), anti-mTOR (catalog no. #2972; Cell Signaling Technology, Inc.), anti-phospho-mTOR (catalog no. #5536; Cell Signaling Technology, Inc.), anti-Beclin1 (catalog no. #3738; Cell Signaling Technology, Inc.), anti-Akt (catalog no. #4691; Cell Signaling Technology, Inc.), anti-phospho-Akt (catalog no. #4060; Cell Signaling Technology, Inc.), and anti-β-actin (catalog no. A5441; Sigma-Aldrich/Merck KGaA) and were incubated overnight at 4˚C. The membranes were subsequently washed and incubated for 1 h with a secondary HRP-conjugated antibody (1:10,000; catalog no. 115-035-144; Jackson ImmunoResearch Inc.). Immunolabeling was performed using an enhanced chemiluminescence detection system (GE Healthcare). The band intensities of the detected proteins (or the phosphorylated proteins) were analyzed via densitometry using the ImageJ software v1.53q (National Institutes of Health) and normalized to those of β-actin. To re-probe the PVDF membranes, the antibodies bound to the membranes were removed by washing twice (15 min each) with a commercial stripping solution and twice (15 min each) with TBS-T, and then the blotted membranes were re-blocked with BSA and re-probed with anti-β-actin antibody.

Immunofluorescence staining. Cells were fixed with 100% methanol for 20 min and then permeabilized using 0.1% Triton X-100 for an additional 30 min. After incubation in

Table I. Monosaccharides used in this study.

Monosaccharides	Category	Molecular weight
D-glucose	Aldohexose	180.16
D-mannose	Aldohexose	180.16
D-allose	Aldohexose	180.16
D-psicose	Ketohexose	180.16
D-tagatose	Ketohexose	180.16
D-sorbose	Ketohexose	180.16
L-psicose	Ketohexose	180.16
D-arabinose	Aldopentose	150.13
L-arabinose	Aldopentose	150.13
L-fucose	Deoxy sugar	164.16

blocking solution (1% BSA in 0.1% Tween 20/PBS) for 1 h, anti-LC3 A/B (1:100; catalog no. #12741; Cell Signaling Technology) and anti-β-actin (1:1,000; catalog no. #A5441; Sigma-Aldrich/Merck KGaA) antibodies diluted in blocking solution were applied and incubated for 1 h at 25˚C. After washing in PBS, the cells were incubated with secondary antibodies (1:1,000; Alexa 568- conjugated anti-rabbit IgG, catalog no. #A31628; and Alexa 488-conjugated anti-mouse IgG, catalog no. A10037; Invitrogen/Thermo Fisher Scientific, Inc.) for 1 h at 25˚C. Nuclei were stained with DAPI (1:1,000; Dojindo Laboratories, Inc.) for 5 min. Immunofluorescence signals were observed using a Keyence BZ-9000 fluorescence microscope (magnification, x600; Keyence Corp.).

Transmission electron microscopy. Cells were fixed with 4% paraformaldehyde and 0.1% glutaraldehyde in 0.1 M phosphate buffer (PB; pH 7.4) for 16 h at 4˚C, and then rinsed three times with 0.1 M PB. Post-fixation was performed with 1% osmium tetroxide/PB for 1 h on ice, and the cells were dehydrated in graded ethanol on ice and embedded in EPON 812 epoxy resin (TAAB) at 60˚C for 72 h. Ultrathin sections (80-100 nm) were cut with an ultramicrotome (EM UC7, Leica Microsystems GmbH) and collected on copper grids. The ultrathin sections were double-stained with uranyl acetate and lead citrate and were subsequently observed on a transmission electron microscope (JEM1400-Flash, JEOL, Ltd.).

RNA extraction and real-time quantitative PCR. Total RNA was extracted from LLC cells using the FastGene™ RNA Basic Kit (Nippon Genetics Co. Ltd.), and the RNA concentration was determined spectrophotometrically (NanoDrop One, Thermo Fisher Scientific, Inc.) at 260 nm. The RNA (500 ng) was then used for first-strand synthesis of cDNA using ReverTra Ace qPCR RT Master Mix (Toyobo Life Science). The following PCR primers were used in this study: *mTOR*, sense, 5'-CTCGCTGATCCAGATGACAA-3' and antisense, 5'-GTCAAGTACACGGGGCAAGT-3'; 18S rRNA, sense, 5'-GGATTGACAGATTGATAGC-3' and antisense, 5'-TAT CGGAATTAACCAGACAA-3'. The mRNA expression levels of *mTOR* and 18S rRNA were quantified via qPCR using a 7900HT Fast Real-Time system (Applied Biosystems/Thermo Fisher Scientific, Inc.). PCR amplification was performed using Sso Advanced SYBR Green Supermix (Bio-Rad Laboratories, Inc.) and data were analyzed using 7900HT software (version 2.3; Applied Biosystems/Thermo Fisher Scientific, Inc.).

Mice. Seven-week-old male C57BL/6J mice (weighing 18.0-22.0 g) were purchased from Charles River Laboratories (Yokohama, Japan). Fifty mice were used in this experiment. Mice were housed in plastic cages (five mice/cage) under controlled conditions of light (12-h light/dark cycle), temperature (23±2˚C), and humidity (55%), and had free access to food and water. The protocols for all animal experiments were approved by the Animal Experimentation Committee of Fujita Health University (approval no. AP19053). Procedures involving mice and their care conformed to international guidelines, as described in the Principles of Laboratory Animal Care (National Institutes of Health publication 85-23, revised 1985 (https://grants.nih.gov/grants/guide/historical/1985_06_25_Vol_14_No_08.pdf).

Tumor xenograft study. C57BL/6J mice were acclimated for one week in a rearing environment. Logarithmic growth phase LLC cells ($5x10^5$ cells/100 μl) were subcutaneously injected into the right posterior flank of each mouse. When the tumor volume reached approximately 50 mm^3, the mice were randomly assigned to four groups. D-allose was orally administered daily at 9 g/kg (D-allose group, n=10) for two weeks as previously described (4), HCQ was intraperitoneally administered at 60 mg/kg every other day (HCQ group, n=10) for two weeks (seven days per two weeks) as described previously (17), and a combination group was also prepared (D-allose + HCQ group, n=10). An untreated group was used as the control (n=9). Tumor volume was measured daily and calculated as 0.5 x length x $width^2$. All mice that reached the study endpoint were euthanized by cervical dislocation under 2-3% isoflurane anesthesia. The humane endpoints were determined as the time where the xenograft tumor diameter was >20 mm, xenograft tumor reached >20% of the animal body weight, body weight loss >20% occurred due to tumor growth, and signs of immobility, inability to eat, ulceration, infection, or necrosis were observed. Death was verified by observation of pupil dilation as well as cessation of breath and heartbeat. Tumor tissues and serum collected from the inferior vena cava were further analyzed.

Measurement of serum D-allose levels. Serum D-allose content in samples was analyzed via HPLC. Briefly, serum samples were mixed (1:1) in 0.6 M perchloric acid. The resulting supernatant (20 μl) was subjected to HPLC analysis. Jusco Finepak GEL SA-121 column (6x100 mm) maintained at 80˚C was used as the anion exchange column. Elution was performed using a gradient of solvent A (0.25 M sodium borate buffer; pH 7.5), and solvent B (0.6 M sodium borate buffer; pH 7.5) at a flow rate of 0.40 ml/min. The gradient changed from 70% A/30% B to 50% A/50% B for 20 min, 50% A/50% B to 0% A/100% B for 1 min; the gradient was maintained at 0% A/100% B for 17 min; and then the gradient changed from 0% A/100% B to 70% A/30% B for 2 min. The eluate from the column was admixed with guanidine-acetonitrile (pH 11.0) at a flow rate of 0.60 ml/min. The resultant effluent was passed

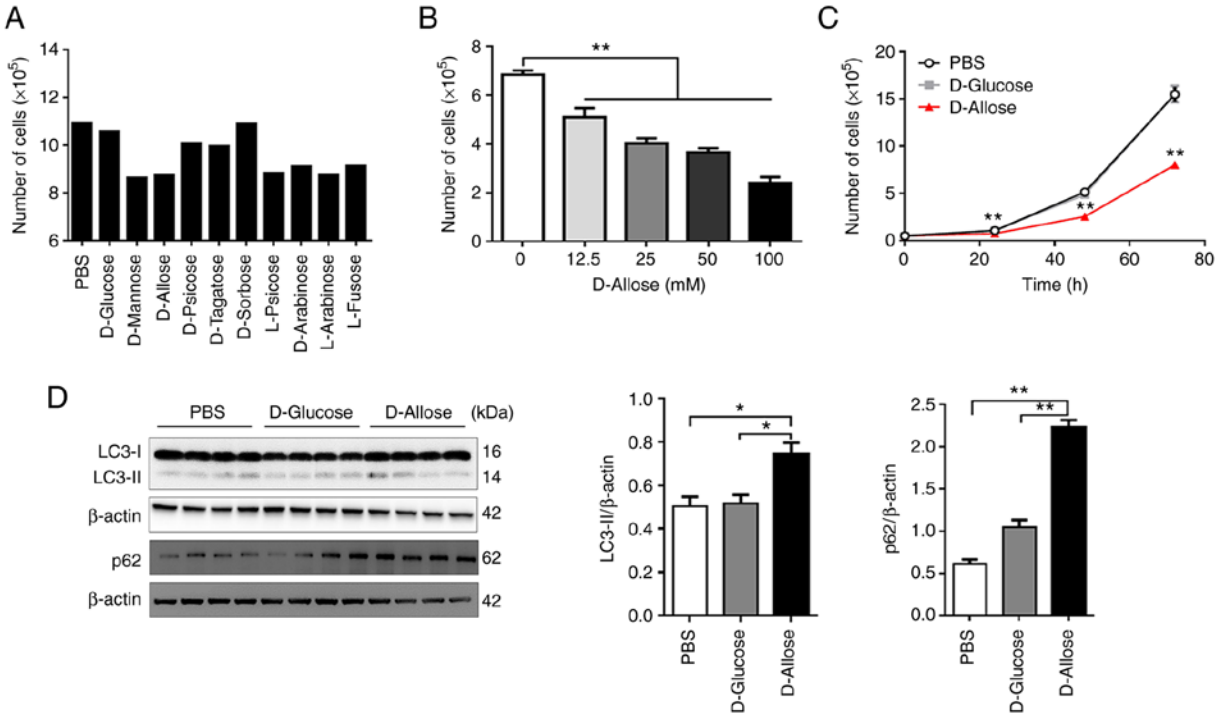

Figure 1. D-allose impairs cell growth and promotes autophagy in LLC cells. LLC cells were cultured for 48 h with or without 25 mM of several monosaccharides. (A and B) The number of live LLC cells was counted using trypan blue staining. (C) Growth curves of LLC cells treated with or without 50 mM D-glucose or 50 mM D-allose. (D) Protein extracts from LLC cells were analyzed by sodium dodecyl sulphate polyacrylamide gel electrophoresis, and immunoblotting was performed using anti-LC3 and anti-p62 antibodies. The results are presented as representative data. The relative densitometric intensities of LC3-II and p62 were determined for each protein band and normalized to that of β-actin. Data are presented as the mean ± SEM. Statistical analysis was performed using (B and D) one-way ANOVA with Tukey's multiple comparison tests or (C) two-way ANOVA with Tukey's multiple comparison test. *P<0.05, **P<0.01. LLC, Lewis lung carcinoma cells.

through a reaction coil maintained at 160˚C and fluorescence was recorded using excitation and emission wavelengths of 310 and 415 nm, respectively.

Histopathology. Tumor tissues were fixed in 10% formalin in PBS overnight. The specimens were embedded in paraffin. Sections that were 4-μm thick were used for hematoxylin and eosin (H&E) staining and immunofluorescence analysis. For immunofluorescence staining sections were incubated in 0.1 M citrate buffer (pH 6.0) for 15 min and heated up to 121˚C using an autoclave. After washing with PBS, sections were incubated in 0.3% hydrogen peroxide and methanol for 30 min to inactivate the endogenous peroxidase. Nonspecific antibody-binding sites were blocked in 2.5% normal horse serum for 30 min. The sections were subsequently incubated with rabbit anti-LC3 A/B antibody (1:1,000; catalog no. #12741; Cell Signaling Technology, Inc.) in PBS and incubated for 1 h at 25˚C. After primary antibody incubation, the sections were rinsed with PBS and incubated with secondary antibody solution (ImmPRESS Reagent, Vector Laboratories, Inc.) for 30 min at 25˚C, followed by the addition of 3,3'-diaminobenzidine tetrahydrochloride (Dako/Agilent Technologies, Inc.). The sections were counterstained with hematoxylin.

Biochemical analysis. Mouse serum glucose (GLU), alanine aminotransferase (ALT), triglyceride (TG), total protein (TP), creatinine (CRE), and blood urea nitrogen (BUN) levels were measured using an automated chemistry analyzer (BioMajesty JCA-BM9130; Jeol Ltd.).

Statistical analysis. All results are expressed as mean ± standard error of the mean (SEM). Significant differences between three or four groups were determined using one-way ANOVA or two-way ANOVA, followed by Tukey's multiple comparison test, and those between two groups were determined using the Student's t-test. A value of P<0.05 was considered significant. All statistical analyses were performed using GraphPad Prism v6.07 (GraphPad Software, Inc.).

Results

D-allose treatment suppresses cell proliferation and promotes autophagy in LLC cells. To evaluate the effect of rare sugars on tumor growth, we cultured LLC cells in the presence of various rare sugars with D-glucose as a control. D-mannose, D-allose, L-psicose, D-arabinose, L-arabinose, and L-fucose suppressed cell growth compared to growth in the presence of PBS or D-glucose (Fig. 1A). D-allose also inhibited the growth of B16F10 mouse melanoma cells (Fig. S1), suggesting that it may suppress the growth of various tumor cells. Therefore, we focused on D-allose in subsequent experiments.

D-allose treatment inhibited LLC cell growth in a significantly dose-dependent manner, and the effect persisted for at least 72 h after treatment (Fig. 1B and C). Notably, a few tumor cells survived in the presence of D-allose (Fig. 1C). It is known that autophagy promotes the survival or resistance of tumor cells to antitumor drugs (18). Therefore, we next examined the expression of LC3-II and p62, both of which are autophagy markers, in D-allose-resistant surviving cells. The

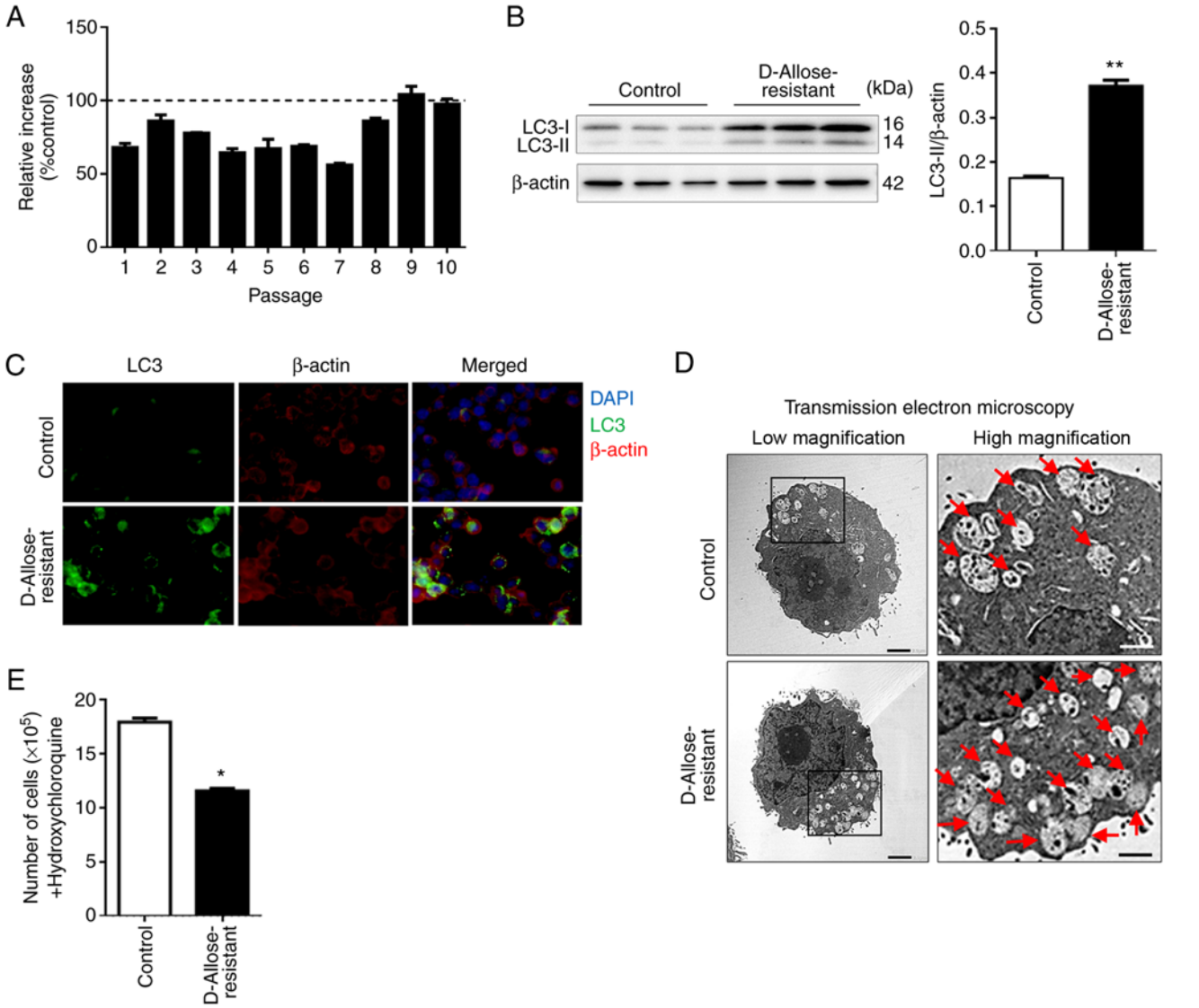

Figure 2. LLC cells surviving under continuous treatment of D-allose promote autophagy and show enhanced susceptibility to autophagy inhibitor hydroxychloroquine. (A) D-allose-resistant LLC cells were established via selection of LLC cells surviving under continuous treatment with 25 mM D-allose. (B) Protein extracts from D-allose-resistant LLC cells were analyzed by sodium dodecyl sulphate polyacrylamide gel electrophoresis, and immunoblotting was performed using anti-LC3 antibodies. The results are presented as representative data (left). The relative densitometric intensity of LC3-II was determined for each protein band and normalized to β-actin (right). (C) LLC cells (control) and D-allose-resistant LLC cells were stained for LC3, β-actin, and 4',6-diamidino-2-phenylindole (nuclei) using immunofluorescence staining. (D) Representative images of transmission electron microscopy of autophagic ultrastructural features in LLC cells (control) and D-allose-resistant LLC cells. Red arrows indicate autolysosomes and autophagosomes. Scale bars, 2.5 μm (left) or 1.0 μm (right). (E) The efficacy of hydroxychloroquine (5 nM) in D-allose-resistant LLC cells was determined by enumerating the live cells using trypan blue staining. Data are presented as the mean ± SEM (n=3). Statistical analysis was performed using paired two-tailed Student's t-test. *P<0.05, **P<0.01 vs. the control group. LLC, Lewis lung carcinoma cells.

expression levels of LC3-II and p62 in surviving LLC cells were significantly increased within 48 h after D-allose treatment (Fig. 1D). Since D-allose has been reported to inhibit the growth of human breast cancer cells (MDA-MB-231) (8), we determined whether autophagy is also involved in the survival of these cells. As expected, D-allose significantly inhibited cell growth and significantly enhanced the expression of LC3-II in the surviving cells (Fig. S2A and B).

D-allose-resistant LLC cells show enhanced autophagy and susceptibility to autophagy inhibitor HCQ. To investigate whether D-allose-induced autophagy is essential for tumor cell survival, we established D-allose-resistant LLC cell lines by selecting only LLC cells that survived in the long-term D-allose cultures. Compared to the untreated control cells, when the proportion of the D-allose-treated LLC cells exceeded 100%, the cells were determined to be D-allose-resistant LLC cells (Fig. 2A). The level of LC3-II in the D-allose-resistant LLC cells was significantly higher than that in the control cells (0.164±0.004 in the control; 0.372±0.012 in the D-allose-resistant LLC cells) (Fig. 2B). Similar results were obtained in the immunohistological analysis (Fig. 2C). Transmission electron microscopic analysis showed increased autolysosomes or autophagosomes (red arrows) in the D-allose-resistant LLC cells (Fig. 2D). Collectively, these results suggest that continuous long-term treatment of LLC cells with D-allose may promote autophagy, leading to tumor survival.

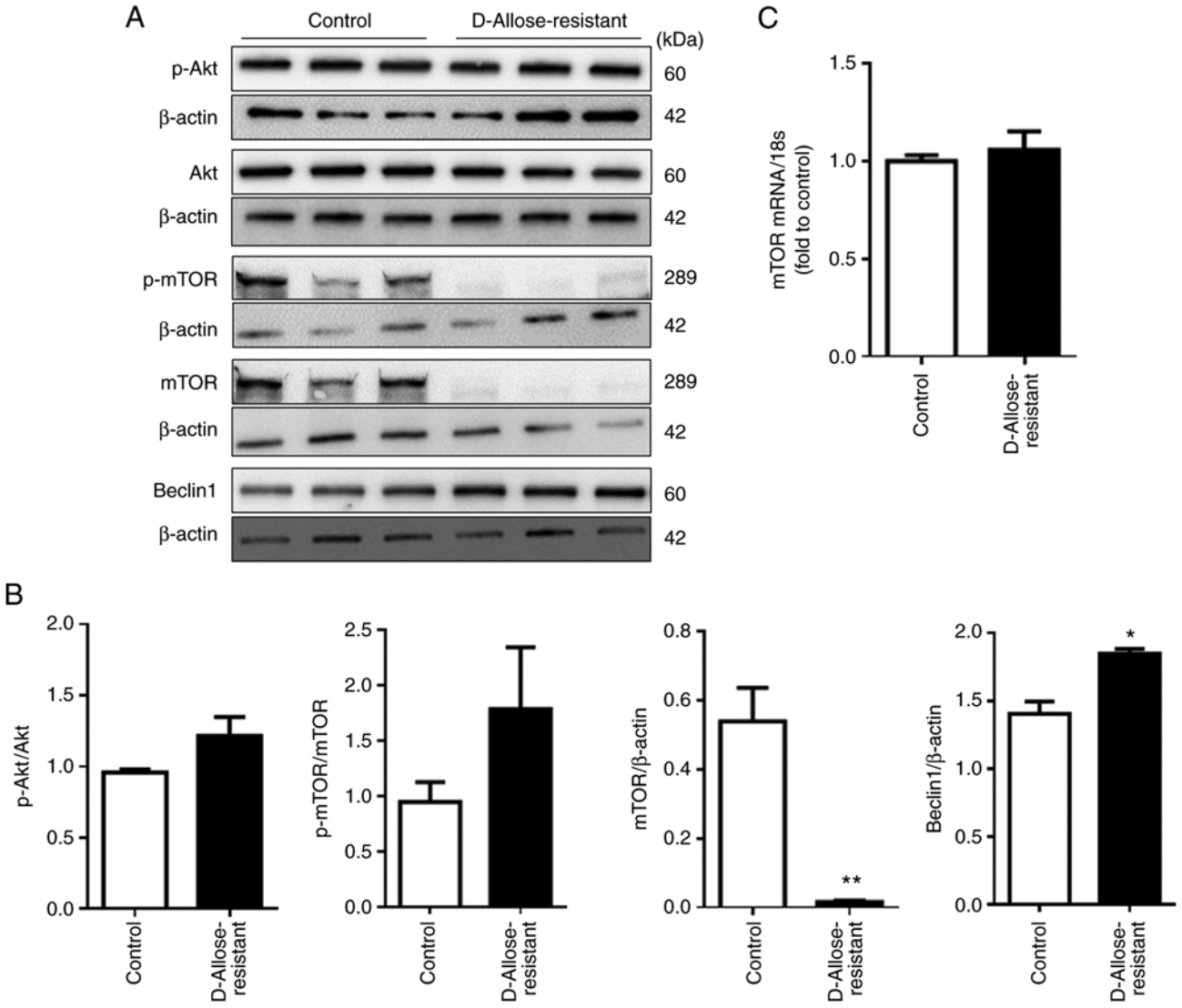

Figure 3. D-allose-resistant LLC cells contain reduced mTOR levels. (A) Protein extracts from LLC cells (control) and D-allose-resistant LLC cells were analyzed by sodium dodecyl sulphate polyacrylamide gel electrophoresis, and immunoblotting was performed using anti-Akt, -p-Akt, -mTOR, -p-mTOR, -Beclin1 and -β-actin antibodies. The results are shown as representative data. (B) The relative densitometric intensity of Akt, p-Akt, mTOR, p-mTOR, and Beclin1 was determined for each protein band and normalized to that of β-actin. (C) The levels of *mTOR* mRNA in LLC cells and D-allose-resistant cells were determined by quantitative polymerase chain reaction. Data are presented as the mean ± SEM (n=3). Statistical analysis was performed using paired two-tailed Student's t-test. $^{*}P<0.05$, $^{**}P<0.01$ vs. the control group. mTOR, mechanistic target of rapamycin; LLC, Lewis lung carcinoma cells.

HCQ, an autophagy inhibitor, is currently studied in phase I and II clinical trials, and more than 20 trials involving HCQ have recruited patients with cancer worldwide. Several studies have shown evidence of preliminary antitumor activity (19,20). Based on clinical reports, we hypothesized that the D-allose-resistant LLC cells may be susceptible to HCQ as an antitumor drug. Upon treatment with HCQ, the viability of D-allose-resistant cells was considerably decreased compared to that of untreated control cells (Fig. 2E). These results suggest that autophagy may be constitutively induced in D-allose-resistant tumor cell lines, thereby enhancing susceptibility to antitumor drugs such as HCQ.

D-allose suppresses the mTOR signaling pathway in LLC cells. Several studies indicate that the mTOR-dependent pathway is a key regulator of autophagy (21,22). Therefore, we investigated the involvement of mTOR in the induction of autophagy in D-allose-resistant LLC cells. The expression of total mTOR and phosphorylated-mTOR (p-mTOR) was detected in the control LLC cells, but was negligible or absent in the D-allose-resistant LLC cells (Fig. 3A and B). The expression of *mTOR* mRNA was not affected (Fig. 3C), implying that D-allose may regulate the expression of mTOR at a post-translational level or induce the proteolytic degradation of mTOR. We also determined the expression of Akt and Beclin1, the upstream and downstream molecules of mTOR, respectively. Although the expression of total Akt and p-Akt was not affected, the expression of Beclin1 was significantly increased in the D-allose-resistant LLC cells (Fig. 3A and B). These results suggest that D-allose-induced autophagy may be mediated by mTOR regulation.

Combination therapy of D-allose and HCQ reduces tumor growth in mice. To determine whether a combination therapy

Table II. Nutritional status, liver function, and renal function in mice after 14 days of treatment.

	Control (No treatment) n=9	D-allose n=10	HCQ n=10	D-allose + HCQ n=10
GLU (mg/dl)	170.0±7.82	174.5±12.44	181.5±11.94	193.5±6.71
ALT (U/l)	10.0±1.57	14.0±2.43	15.5±1.80	17.5±3.69
TG (mg/dl)	183.9±53.57	212.5±32.33	131.5±31.50	217.5±56.90
TP (g/dl)	5.11±0.19	5.30±0.14	5.65±0.17	5.53±0.05
CRE (mg/dl)	0.14±0.01	0.15±0.01	0.15±0.00	0.14±0.01
BUN (mg/dl)	33.06±1.93	32.05±2.14	32.25±1.79	30.05±1.27

Data are presented as the mean ± SEM (n=9-10) and analyzed via one-way ANOVA with Tukey's multiple comparison test. HCQ, hydroxychloroquine; GLU, glucose; ALT, alanine aminotransferase; TG, triglyceride; TP, total protein; CRE, creatinine; BUN, blood urea nitrogen.

of D-allose and HCQ shows enhanced antitumor activity *in vivo*, we administered D-allose with or without HCQ into LLC-implanted mice for 14 consecutive days. The levels of GLU, ALT, TG, TP, CRE, and BUN in the sera were found to be normal (Table II), and weight loss was not observed in any group (Fig. 4A), indicating that there were no side effects of the combination therapy of D-allose and HCQ for at least 14 days. Tumor volume and gross findings in D-allose + HCQ-treated mice were significantly reduced compared to that in the untreated control, D-allose-, or HCQ-treated mice (Fig. 4B and C). Similar results were obtained in an *in vitro* culture system (Fig. S3). We found significantly increased D-allose levels in the sera and LC3-II expression at the tumor site in D-allose-treated mice implanted with LLC cells (Fig. 4D-G). These results suggest that established D-allose-resistant LLC cells constitutively induce autophagy, thereby enhancing the sensitivity to autophagy inhibitors.

Discussion

In the present study, we found that D-allose inhibited the growth of various tumor cells including mouse- and human-derived tumor cells and induced autophagy in the surviving cells. Furthermore, the enhanced autophagy in the established D-allose-resistant tumor cells was associated with increased sensitivity to hydroxychloroquine (HCQ), leading to the induction of autophagic cell death. These results indicate that the combination of D-allose and HCQ can significantly inhibit tumor growth in a mouse tumor-bearing model without causing significant side effects.

Autophagy is induced by several pathways via mTOR signaling, including the PI3K/AKT (23), p53 (24), amino acid, Rag GTPase-mediated (25,26), and MAPK/ERK (27) signaling pathways. Glucose deprivation induces growth inhibition and death of tumor cells in a mTOR-mediated autophagy-dependent manner (15,28). Paradoxically, it has been reported that exposure to high glucose downregulates glucose transporter 1 (GLUT1) expression, leading to growth inhibition of tumor cells (29). Interestingly, under high glucose conditions, thioredoxin-interacting protein (TXNIP) expression was found to be enhanced in a retinal muller cell line, which induced mTOR-mediated autophagy (30), suggesting that the induction of autophagy is dependent on abnormal glucose microenvironments. Importantly, D-allose was found to reduce the expression of GLUT1 via upregulation of TXNIP in tumor cells, thereby inhibiting tumor growth through impaired glucose uptake (8,9). However, D-allose-driven inhibition of glucose uptake cannot completely kill tumor cells *in vitro* and *in vivo* (10). Based on these findings, we speculated that, upon stimulation with D-allose, a small number of tumor cells can survive in a glucose-independent manner through the induction of autophagy, and we found that D-allose induces mTOR-mediated autophagy in surviving tumor cells. Therefore, our findings shed new light on the role of D-allose-induced autophagy in tumor cell survival, which obviously differs from recent reports that D-allose induces tumor cell death (8-10). Collectively, D-allose-resistant tumor cells, which presumably exhibit impaired TXNIP-mediated GLUT1 expression, may survive using intracellular glucose produced through the autophagic processing of cellular components. Here, we found that mTOR protein levels were decreased in D-allose-resistant LLC cells without any change in *mTOR* mRNA levels. There are two possible mechanisms that explain the selective downregulation of mTOR at the protein level: i) the post-transcriptional modification of mTOR is impaired, or ii) mTOR protein is proteolytically processed. Regarding the latter mechanism, gephyrin, a neuronal receptor assembly protein, reduces the level of protein, but not mRNA, of mTOR in lung squamous cell carcinoma by promoting ubiquitin-dependent degradation (31). In addition, in mouse liver tumor cells, mTOR signaling in $CD133^+$ cancer stem cells was found to be less active than that in $CD133^-$ non-stem cancer cells (32). These findings suggest that D-allose kills $mTOR^+$ tumor cells, thereby permitting the survival of $mTOR^-$ tumor cells, which may explain our findings that mTOR protein selectively disappeared in D-allose-resistant cells. Although we could not determine the mechanism by which D-allose induces the downregulation of mTOR protein, few studies indicate that the mTOR signaling pathways are abnormally regulated in most human cancers (33,34).

We showed that the D-allose-induced downregulation of mTOR protein is positively correlated with the upregulation of LC-II and Beclin1 as well as the increased number of autophagosomes in the resistant Lewis lung carcinoma (LLC) cells, and the sensitivity to HCQ in the resistant LLC cells was enhanced, indicating that D-allose-induced autophagy not

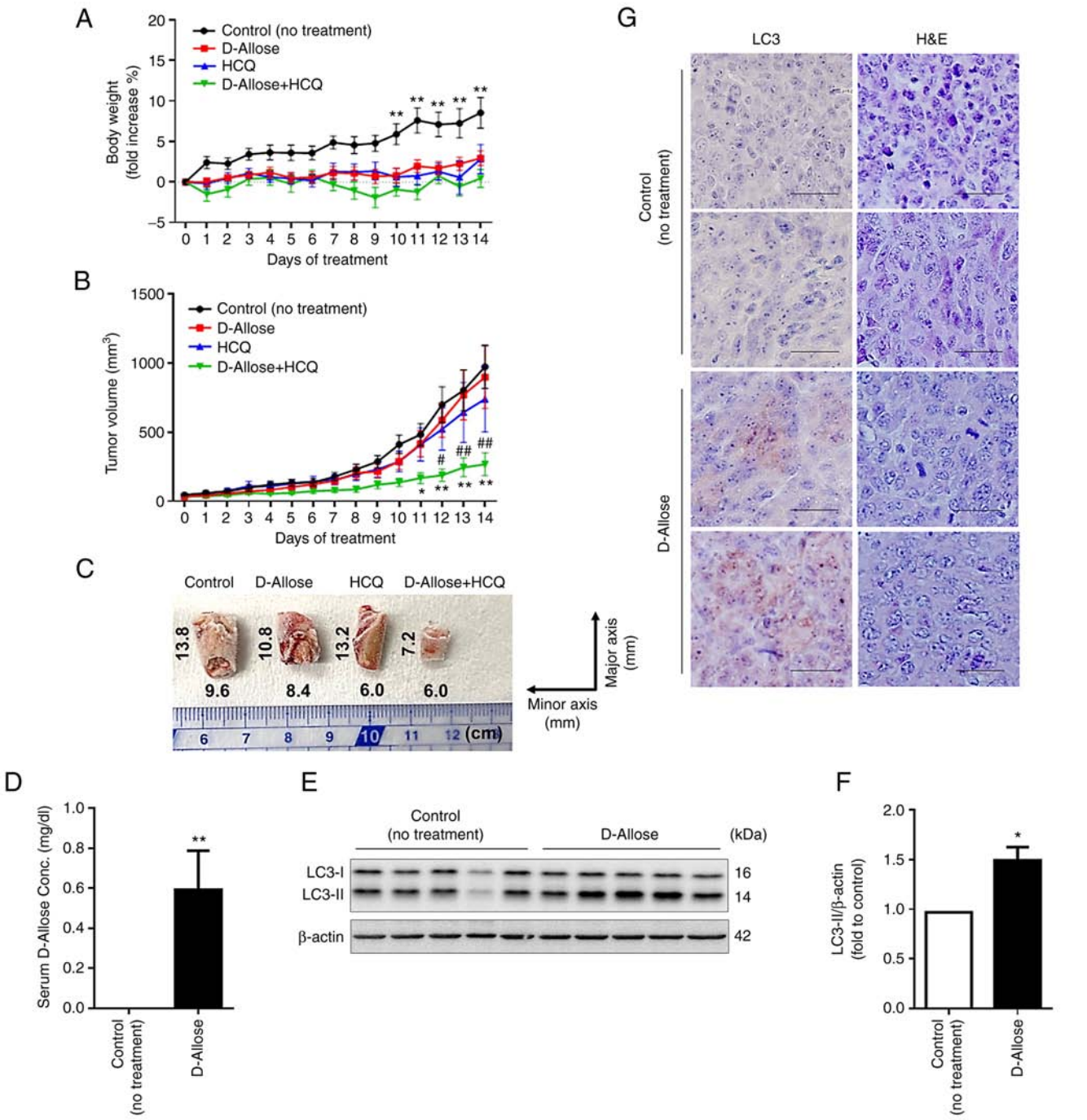

Figure 4. Combination therapy of D-allose and hydroxychloroquine (HCQ) reduces LLC cell growth in mice. Changes in (A) body weight and (B) tumor growth curves in LLC xenograft mice following initiation of treatment without (control, n=9) or with D-allose (9 g/kg, n=10), HCQ (60 mg/kg, n=10), and a combination of D-allose (9 g/kg) and HCQ (60 mg/kg) (n=10). Data are presented as the mean ± SEM. Statistical analysis was performed using two-way ANOVA with Tukey's multiple comparison test. *P<0.05, **P<0.01 vs. the control, $^{\#}$P<0.05, $^{\#\#}$P<0.01 vs. HCQ treatment. (C) Representative images of frozen tumor tissues (cut in the half size) of indicated mice 14 days after treatment are shown. (D) Serum D-allose levels in control and D-allose-treated mice 14 days after treatment were measured by high-performance liquid chromatography. **P<0.01 vs. the control. (E and F) Expression levels of LC3-II in the tumor tissues of control and D-allose-treated mice 14 days after treatment. The results are presented as representative data (left). The relative densitometric intensity of LC3-II was determined for each protein band and normalized to that of β-actin (right). Data are presented as the mean ± SEM. Statistical analysis was performed using a paired two-tailed Student's t-test. *P<0.05 vs. the control. (G) LC-3 in tumor sites of control and D-allose-treated mice 14 days after treatment was detected using immunohistochemistry staining. Hematoxylin and eosin (H&E) staining results are shown in the right column. HCQ, hydroxychloroquine; LLC, Lewis lung carcinoma.

only is essential for their survival but is also a promising therapeutic target. Our findings raise a question regarding which cells acquire resistance against D-allose via the induction of autophagy. Based on this aspect, it is known that autophagy is induced constitutively and predominantly in cancer stem cells to maintain their survival and pluripotency (35). These findings suggest that D-allose kills cancer cells, which are presumably non-stem cells, via inhibition of glucose uptake and selectively supports cancer stem cells via the induction of autophagy. However, the relationship between D-allose and

mTOR signaling in the induction of autophagy remains unclear. Further studies are required to elucidate this relationship.

We also found that LLC cell proliferation was considerably inhibited in the D-allose and HCQ co-treatment group compared to that in the control and HCQ groups. Based on our findings, we propose that D-allose kills non-stem cancer cells and sensitizes surviving cancer stem cells to HCQ chemotherapy, leading to the suppression of tumor growth. Candidate autophagy inhibitors for cancer treatment include bafilomycin A1, 3-methyladenine, chloroquine (CQ), and HCQ, among which HCQ is currently undergoing phase II clinical trials (19). Indeed, autophagy induced by gefitinib and paclitaxel, both of which are antitumor drugs for non-small cell lung cancer, increases cytotoxicity when these drugs are combined with CQ and HCQ treatments (36,37) and the combination of HCQ and ixabepilone, an antitumor drug, showed improved therapeutic efficacy against breast cancer (38). Rapamycin, an mTOR inhibitor, has been reported to suppress the growth of tumor cells by inducing autophagy (39). In contrast, the combination of CQ and cisplatin, a chemotherapeutic drug, has been reported to induce damage in healthy kidneys, suggesting that autophagy plays a protective role in normal renal cells (40). Therefore, D-allose-induced autophagy may possess both tumoricidal activity against various cancer cells and protective activity against normal cells, and the combined use of D-allose and autophagy inhibitors may be safer and more selective than that of D-allose and chemoradiotherapy in the induction of antitumor activity (10).

This study provides a new therapeutic strategy that targets autophagy induced in tumor cells by D-allose administration. Notably, D-allose, which has various physiological functions, can be mass-produced industrially; however, there are no studies focusing on autophagy in tumor cells. Therefore, the new information on D-allose found in this study will contribute to improving the therapeutic response in combination with clinically applied autophagy inhibitors.

Acknowledgements

Not appliable.

Funding

This study was funded by Matsutani Chemical Industry Co., Ltd.

Availability of data and materials

The datasets used and/or analyzed during the current study are available from the corresponding author upon reasonable request.

Authors' contributions

MHo and KS planned the experiments. KY, MHo, HT, NM, MHi, SY, and FS performed the experiments. KY, MHo, and HT were responsible for data integrity and data analysis. KY, MHo, HT, NM, MHi, FS, SY, and KS discussed the results. KY, MHo, and HT wrote the manuscript. KY, MHo, HT, NM, MHi, FS, SY, and KS conducted the research. KY and MHo confirm the authenticity of all the raw data. KS had primary responsibility for the final content. All authors read and approved the final manuscript for publication.

Ethics approval and consent to participate

The protocols for all animal experiments were approved by the Animal Experimentation Committee of Fujita Health University (approval no. AP19053).

Patient consent for publication

Not applicable.

Competing interests

Kyoka Yamazaki is an employee of Matsutani Chemical Industry Co., Ltd. Kuniaki Saito was funded by A&T Corporation, Nisshin Seifun Group, Marukome Corporation, and Tsuji-seiyu Corporation and belongs to an endowed chair funded by Fujifilm Wako Pure Chemical Corporation and A&T Corporation. The other authors have no financial competing interests.

References

1. Sung H, Ferlay J, Siegel RL, Laversanne M, Soerjomataram I, Jemal A and Bray F: Global cancer statistics 2020: GLOBOCAN estimates of incidence and mortality worldwide for 36 cancers in 185 countries. CA Cancer J Clin 71: 209-249, 2021.
2. Siegel RL, Miller KD and Jemal A: Cancer statistics, 2020. CA Cancer J Clin 70: 7-30, 2020.
3. Mooradian AD, Smith M and Tokuda M: The role of artificial and natural sweeteners in reducing the consumption of table sugar: A narrative review. Clin Nutr ESPEN 18: 1-8, 2017.
4. Iga Y, Nakamichi K, Shirai Y and Matsuo T: Acute and sub-chronic toxicity of D-allose in rats. Biosci Biotechnol Biochem 74: 1476-1478, 2010.
5. Yamada T, Iida T, Takamine S, Hayashi N and Okuma K: Safety evaluation of rare sugar syrup: Single-dose oral toxicity in rats, reverse mutation assay, chromosome aberration assay, and acute non-effect level for diarrhea of a single dose in humans. Shokuhin Eiseigaku Zasshi 56: 211-216, 2015 (In Japanese).
6. Liu Y, Nakamura T, Toyoshima T, Shinomiya A, Tamiya T, Tokuda M, Keep RF and Itano T: The effects of D-allose on transient ischemic neuronal death and analysis of its mechanism. Brain Res Bull 109: 127-131, 2014.
7. Yamaguchi F, Takata M, Kamitori K, Nonaka M, Dong Y, Sui L and Tokuda M: Rare sugar D-allose induces specific up-regulation of TXNIP and subsequent G1 cell cycle arrest in hepatocellular carcinoma cells by stabilization of p27kip1. Int J Oncol 32: 377-385, 2008.
8. Noguchi C, Kamitori K, Hossain A, Hoshikawa H, Katagi A, Dong Y, Sui L, Tokuda M and Yamaguchi F: D-allose inhibits cancer cell growth by reducing GLUT1 expression. Tohoku J Exp Med 238: 131-141, 2016.
9. Hoshikawa H, Mori T and Mori N: In vitro and in vivo effects of D-allose: Up-regulation of thioredoxin-interacting protein in head and neck cancer cells. Ann Otol Rhinol Laryngol 119: 567-571, 2010.
10. Hoshikawa H, Kamitori K, Indo K, Mori T, Kamata M, Takahashi T and Tokuda M: Combined treatment with D-allose, docetaxel and radiation inhibits the tumor growth in an in vivo model of head and neck cancer. Oncol Lett 15: 3422-3428, 2018.
11. Balamurugan K: HIF-1 at the crossroads of hypoxia, inflammation, and cancer. Int J Cancer 138: 1058-1066, 2016.
12. Rabinowitz JD and White E: Autophagy and metabolism. Science 330: 1344-1348, 2010.
13. Heitman J, Movva NR and Hall MN: Targets for cell cycle arrest by the immunosuppressant rapamycin in yeast. Science 253: 905-909, 1991.

14. Noda T and Ohsumi Y: Tor, a phosphatidylinositol kinase homologue, controls autophagy in yeast. J Biol Chem 273: 3963-3966, 1998.
15. Kim J, Kundu M, Viollet B and Guan KL: AMPK and mTOR regulate autophagy through direct phosphorylation of Ulk1. Nat Cell Biol 13: 132-141, 2011.
16. Mathew R, Karantza-Wadsworth V and White E: Role of autophagy in cancer. Nat Rev Cancer 7: 961-967, 2007.
17. Gao L, Wang Z, Lu D, Huang J, Liu J and Hong L: Paeonol induces cytoprotective autophagy via blocking the Akt/mTOR pathway in ovarian cancer cells. Cell Death Dis 10: 609, 2019.
18. Sui X, Chen R, Wang Z, Huang Z, Kong N, Zhang M, Han W, Lou F, Yang J, Zhang Q, *et al*: Autophagy and chemotherapy resistance: A promising therapeutic target for cancer treatment. Cell Death Dis 4: e838, 2013.
19. Chude CI and Amaravadi RK: Targeting autophagy in cancer: Update on clinical trials and novel inhibitors. Int J Mol Sci 18: 127, 2017.
20. Amaravadi RK, Lippincott-Schwartz J, Yin XM, Weiss WA, Takebe N, Timmer W, DiPaola RS, Lotze MT and White E: Principles and current strategies for targeting autophagy for cancer treatment. Clin Cancer Res 17: 654-666, 2011.
21. Nicklin P, Bergman P, Zhang B, Triantafellow E, Wang H, Nyfeler B, Yang H, Hild M, Kung C, Wilson C, *et al*: Bidirectional transport of amino acids regulates mTOR and autophagy. Cell 136: 521-534, 2009.
22. Yu L, McPhee CK, Zheng L, Mardones GA, Rong Y, Peng J, Mi N, Zhao Y, Liu Z, Wan F, *et al*: Termination of autophagy and reformation of lysosomes regulated by mTOR. Nature 465: 942-946, 2010.
23. Kim YC and Guan KL: mTOR: A pharmacologic target for autophagy regulation. J Clin Invest 125: 25-32, 2015.
24. Mrakovcic M and Frohlich LF: p53-mediated molecular control of autophagy in tumor cells. Biomolecules 8: 14, 2018.
25. Kim E, Goraksha-Hicks P, Li L, Neufeld TP and Guan KL: Regulation of TORC1 by Rag GTPases in nutrient response. Nat Cell Biol 10: 935-945, 2008.
26. Sancak Y, Bar-Peled L, Zoncu R, Markhard AL, Nada S and Sabatini DM: Ragulator-Rag complex targets mTORC1 to the lysosomal surface and is necessary for its activation by amino acids. Cell 141: 290-303, 2010.
27. Corcelle E, Djerbi N, Mari M, Nebout M, Fiorini C, Fenichel P, Hofman P, Poujeol P and Mograbi B: Control of the autophagy maturation step by the MAPK ERK and p38: Lessons from environmental carcinogens. Autophagy 3: 57-59, 2007.
28. Matsui Y, Takagi H, Qu X, Abdellatif M, Sakoda H, Asano T, Levine B and Sadoshima J: Distinct roles of autophagy in the heart during ischemia and reperfusion: roles of AMP-activated protein kinase and Beclin 1 in mediating autophagy. Circ Res 100: 914-922, 2007.
29. Jozwiak P, Krzeslak A, Bryś M and Lipinska A: Glucose-dependent glucose transporter 1 expression and its impact on viability of thyroid cancer cells. Oncol Rep 33: 913-920, 2015.
30. Ao H, Li H, Zhao X, Liu B and Lu L: TXNIP positively regulates the autophagy and apoptosis in the rat muller cell of diabetic retinopathy. Life Sci 267: 118988, 2021.
31. Zhang X, Cheng D, Liu Y, Wu Y and He Z: Gephyrin suppresses lung squamous cell carcinoma development by reducing mTOR pathway activation. Cancer Manag Res 11: 5333-5341, 2019.
32. Yang Z, Zhang L, Ma A, Liu L, Li J, Gu J and Liu Y: Transient mTOR inhibition facilitates continuous growth of liver tumors by modulating the maintenance of CD133+ cell populations. PLoS One 6: e28405, 2011.
33. Kenerson HL, Aicher LD, True LD and Yeung RS: Activated mammalian target of rapamycin pathway in the pathogenesis of tuberous sclerosis complex renal tumors. Cancer Res 62: 5645-5650, 2002.
34. Inoki K, Corradetti MN and Guan KL: Dysregulation of the TSC-mTOR pathway in human disease. Nat Genet 37: 19-24, 2005.
35. Nazio F, Bordi M, Cianfanelli V, Locatelli F and Cecconi F: Autophagy and cancer stem cells: Molecular mechanisms and therapeutic applications. Cell Death Differ 26: 690-702, 2019.
36. Han W, Pan H, Chen Y, Sun J, Wang Y, Li J, Ge W, Feng L, Lin X, Wang X, *et al*: EGFR tyrosine kinase inhibitors activate autophagy as a cytoprotective response in human lung cancer cells. PLoS One 6: e18691, 2011.
37. Chen K and Shi W: Autophagy regulates resistance of non-small cell lung cancer cells to paclitaxel. Tumour Biol 37: 10539-10544, 2016.
38. Ojha R, Bhattacharyya S and Singh SK: Autophagy in cancer stem cells: A potential link between chemoresistance, recurrence, and metastasis. Biores Open Access 4: 97-108, 2015.
39. Chi KH, Ko HL, Yang KL, Lee CY, Chi MS and Kao SJ: Addition of rapamycin and hydroxychloroquine to metronomic chemotherapy as a second line treatment results in high salvage rates for refractory metastatic solid tumors: A pilot safety and effectiveness analysis in a small patient cohort. Oncotarget 6: 16735-16745, 2015.
40. Kimura T, Takabatake Y, Takahashi A and Isaka Y: Chloroquine in cancer therapy: A double-edged sword of autophagy. Cancer Res 73: 3-7, 2013.